Role of the Crystal-Field Theory in Determining the Structures of Spinels

Jeremy K. Burdett,*[1a,b] Geoffrey D. Price,[1c] and Sarah L. Price[1b]

Contribution from the Departments of Chemistry and Geophysical Sciences, The University of Chicago, Chicago, Illinois 60637. *Received April 8, 1981*

Abstract: Pseudo-potential orbital radii r_s, r_p are used to construct an index $r_\sigma = r_s + r_p$. A plot of r_σ^A vs. r_σ^B for 172 chalconide spinels (AB_2X_4) leads to two well-defined areas which contain only normal or inverse spinels, with only four errors. At the boundary of the two regions the observed structures are generally in agreement with crystal-field ideas. The gross sorting is achieved without recourse either to the number of d electrons or an orbital radius r_d, which implies that it is the A,B s- and p-orbital energies which primarily determine coordination numbers in these systems. In fact, whereas d-orbital-based crystal-field ideas are only practically applicable to 74 transition metal containing examples of our data base (of which only 61, or 82%, are predicted correctly as normal or inverse variants), good structural sorting is achieved for all examples using r_σ plots (a 98% success rate). The relative (minor) importance of d orbitals and (major) importance of higher energy s, p orbitals on A,B is thus in accord with the relative energetic importance of these orbitals in ligand coordination. For the first time the reasons determining site preferences of non-transition-metal ions are identified.

Introduction

The spinels, crystalline solids of general formula AB_2X_4, have been known for many years and are well known[2] to mineralogists, chemists, and solid-state physicists. A,B may be either d- or f-block metals; group 1A,B or 2A,B metals; or group 3A or 4A atoms. Species with formal oxidation states $A^{II}B^{III}X_4$, $A^{IV}B_2^{III}X_4$, and $A^{VI}B_2^{I}X_4$ are known. X is usually oxygen (but examples are known with all the stable chalcogens) or halogen. Related species exist containing the pseudo-halogen CN^-. The structures may be described as based on a cubic close-packed array of X^{2-} ions (for the chalcogens) with the A,B ions occupying the interstices in the structure. In the normal structure the A ions (atoms) occupy one-eighth of the tetrahedral sites and the B ions one-half of the octahedral sites ($\{A\}[B_2]X_4$ where the brackets represent octahedral and the braces tetrahedral site occupations). In the inverse structure all the A atoms and one-half of the B atoms have exchanged places, $[A]\{B\}[B]X_4$. This interesting site preference problem, namely, when is $\{A\}[B]$ more stable than $[A]\{B\}$, has attracted attention for many years. When either one or both out of A and B are transition metals, one of the traditional approaches to the problem has been the application[3] of the d-orbital-based crystal-field theory (CFT) which allows computation of an octahedral site preference energy (OSPE) for each ion. This is the difference between crystal-field stabilization energies (CFSE) for octahedral and tetrahedral coordination in terms of the d-electron configuration of the ion and the cubic parameter Dq. The latter is available numerically for most ions from studies of the electronic spectra of cubically coordinated A and B ions. In this scheme the ion with the larger OSPE will occupy the octahedral sites and hence specify whether the structure is normal or inverse. Such discussions have been textbook material for $1^1/_2$ decades.[4a] CFT ideas have, in fact, played a major theoretical role in this area. Although other theories, particularly evaluation of the Madelung[5,6] energy, have been proposed to explain the cation distribution, a thorough treatment sums both Madelung energy and crystal-field effects. However, the conceptual simplicity of the CFT approach has led to an undue emphasis, perhaps, on its role in determining cation distribution. In this report we shall describe a rival scheme which not only sorts inverse and normal spinels more accurately but is just as applicable to those cases where CFT makes no predictions as in some transition metal examples and in all species containing closed d shells. These examples, where no predictions can be made, make up over 60% (for oxide spinels) of the available examples. Importantly we identify the conditions under which crystal-field considerations may be of importance.

Structural Sorting Maps

If we wish to decide which of two structural alternatives for a class of molecular or solid-state systems is more stable, an obvious route to take is one which involves direct numerical computation via the laws of quantum mechanics. For most solid-state systems this capability is at present beyond us. One method currently receiving considerable interest[7] is the use of structural sorting maps. By plotting one judiciously chosen parameter for A and B against another, for the AB binaries, for example, well-defined regions are found in such a two-dimensional display in which all examples of one structural type are found. Mooser–Pearson diagrams[8] use as such structural indices the average value of the principal valence quantum number for A and B and their Pauling electronegativity difference. More recent maps have used[7,10] two completely quantum mechanical indexes in combinations of so-called "orbital radii", r_l ($l = 0, 1, 2$), which are the crossing points of the nonlocal pseudo-potential $V_{\text{eff}}^l(r)$. The r_l may be evaluated either from first principles[10g,h] or from atomic spectral data[10a,b] and have several interesting properties.[11] They scale inversely with the corre-

(1) (a) Fellow of the Alfred P. Sloan Foundation and Camille and Henry Dreyfus Teacher-Scholar. (b) Department of Chemistry. (c) Department of Geophysical Sciences.

(2) For reviews and compilations of known examples, see: (a) Muller, O.; Roy, R. "The Major Ternary Structural Families"; Springer-Verlag: New York, 1974. (b) Hill, R. J.; Craig, J. R.; Gibbs, G. V. *Phys. Chem. Miner.* **1979**, *4*, 317. (c) Wyckoff, R. W. G. "Crystal Structures"; Wiley: New York, 1965.

(3) (a) Dunn, T. M.; McClure, D. S.; Pearson, R. G. "Some Aspects of Crytal Field Theory"; Harper & Row: New York, 1965. (b) McClure, D. S. *J. Phys. Chem. Solids* **1957**, *3*, 311. (c) Dunitz, J. D.; Orgel, L. E. *Ibid.* **1957**, *3*, 318. (d) Dunitz, J. D.; Orgel, L. E. *Adv. Inorg. Chem. Radiochem.* **1960**, *3*, 1. (e) Burns, R. G. "Mineralogical Applications of Crystal Field Theory"; Cambridge University Press: New York, 1970. (f) Navrotsky, A.; Kleppa, O. J. *J. Inorg. Nucl. Chem.* **1967**, *29*, 2701; **1968**, *30*, 479.

(4) Cotton, F. A.; Wilkinson, G. "Advanced Inorganic Chemistry", Wiley: New York: (a) 2nd ed.; 1966; (b) 4th ed., 1980.

(5) Miller, A. *J. Appl. Phys.* (*Suppl.*) **1959**, *30*, 24S.

(6) Verwey, E. J. W.; De Boer, F.; Santen, J. H. *J. Chem. Phys.* **1948**, *16*, 1091.

(7) (a) Burdett, J. K. *Adv. Chem. Phys.*, in press. (b) Phillips, J. C. *Commun. Solid State Phys.* **1978**, *9*, 11. (c) Navrotsky, A.; O'Keeffe, M., Eds. "Structure and Bonding in Crystals"; Academic Press: New York, 1981.

(8) (a) Mooser, E.; Pearson, W. B. *Acta Crystallogr.*, **1959**, *12*, 1015. (b) Pearson, W. B. *J. Phys. Chem. Solids* **1962**, *23*, 103. (c) This too is now textbook material; see ref 9.

(9) Huheey, J. E. "Inorganic Chemistry"; Harper & Row: New York, 1978.

(10) (a) Simons, G.; Bloch, A. N. *Phys. Rev. B* **1973**, *7*, 2754. (b) St. John, J.; Bloch, A. N. *Phys. Rev. Lett.* **1974**, *33*, 1095. (c) Zunger, A.; Cohen, M. L. *Ibid.* **1978**, *41*, 53. (d) Zunger, A. *Ibid.* **1980**, *44*, 582. (e) Zunger, A. *Phys. Rev. B* **1980**, *22*, 5839. (f) Machlin, E. S.; Chow, T. P.; Phillips, J. C. *Phys. Rev. Lett.* **1977**, *38*, 1292. (g) Phillips, J. C.; Chelikowsky, J. R. *Phys. Rev. B* **1978**, *17*, 2453. (h) Burdett, J. K.; Price, S. L. *Ibid.* **1981**, *22*, 5462.

0002-7863/82/1504-0092$01.25/0

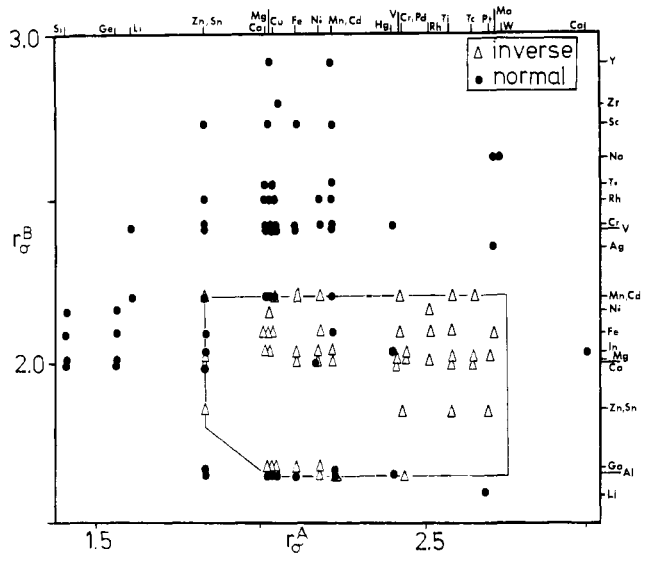

Figure 1. Structural sorting map for AB_2X_4 chalconide spinels, using r_σ^A and r_σ^B as indexes. Not shown are the lanthanide examples which all have the normal structure. The value of r_σ^B for La lies off the top of the plot, and thus all such spinels fall in the normal region of the maps. (This assumes similar radii for all the lanthanides.) Many points on this plot represent more than one spinel because (a) we do not distinguish the nature of X and (b) the proximity of r_σ for some of the elements, e.g., Cr, Pd, and Mn, Cd.

Table I

I.	CFT approach
	(a) data base size = 172
	(b) number of examples with transition metals = 156
	(c) number with only d^0, d^5, d^{10} transition metal ions = 53
	(d) number of examples where data are not available[a] = 29
	(e) number of cases where CFT can make a prediction = 74
	(f) number of successes by CFT = 61 (82% of c[b] or 42% of a-d)
II.	structural map
	(a) data base size = 172
	(b) number of successes = 168 (98%)[c]
III.	crystal radii
	(a) data base size = 48

[a] The values for the OSPE are taken from ref 3a but electronic spectral data are not available for some ions (e.g., Tc^{3+}). We assume that the relative size of the OSPE's is the same for X = S, Se, Te as for X = O. [b] This is the best success rate we can achieve and includes making the assumption, for example, that $FeCo_2O_4$ and $MnCo_2O_4$ are really $Co^{II}Fe^{III}Co^{III}O_4$ and $Co^{II}Mn^{III}Co^{III}O_4$ which are compatible with the relative ionization potentials for $M^{2+} \rightarrow Mn^{3+}$ for Mn, Fe, and Co. If it is assumed in addition that there is an error of ±5 kcal mol^{-1} in estimating the CFSE's, then the number of "errors" decreases. The best subset of examples which the CFT treats are the II, III oxide spinels which, with this assumption, are predicted with only one "error" in 32. [c] Neglecting the "borderline" examples which CFT is able to treat.

sponding orbital ionization energies, i.e., $r_0^{-1} = r_s^{-1} \propto H_{ss}$ and $r_1^{-1} = r_p^{-1} \propto H_{pp}$, and thus a weighted sum of the r_l^{-1} may be used as an estimate of electronegativity in the spirit of Mulliken's definition. $r_\sigma = r_s + r_p$ is also closely correlated with Pauling's tetrahedral atomic radius and thus is a measure of the "size" of the atom or ion.

In Figure 1 we present a structural map for the known chalcogenide spinels (with A ≠ B), included irrespective of the atom type A,B (and their electron count, oxidation state, etc.) using as indexes the two parameters $r_\sigma^A = r_s^A + r_p^A$ and $r_\sigma^B = r_s^B + r_p^B$, and the first-principles radii of Zunger.[10e] The sorting is very good indeed with only four obvious errors: $CdFe_2O_4$, $MnFe_2O_4$, $NiCo_2S_4$, and $HgIn_2S_4$ in a data base of 172. A breakdown of the data base is shown in Table I. An analogous sorting is achieved (with the same errors) if the electronegativity functions $\chi^A = r_s^{A-1} + r_p^{A-1}$, $\chi^B = r_s^{B-1} + r_p^{B-1}$ are used. This sorting is quite impressive and appears to be independent of the nature of X. Although in principle there are four errors according to the compendia of ref 2, the evidence for the assignment of normal character is not always very good. For $HgIn_2S_4$ the assignment is based on powder diffraction data[12] and is not very reliable, and similarly for $CdFe_2O_4$ we need to rely on an old X-ray diffraction determination.[13] Only for $MnFe_2O_4$ and $NiCo_2S_4$ are there good, modern (neutron) studies[14] which unequivocally confirm the normal structure.

Table II. Crystal-Field Stabilization Energies of Borderline Spinels, $(A_{1-x}B_x)[A_xB_{2-x}]O_4$[a]

B	A	x[b]	OSPE(A-B), kcal mol^{-1}
Al	Fe	0.0	3.9
	Mg	0.07-0.1	0.0
	Co	0.2	2.1
	Mn	0.3	0.0
	Cu	0.4-0.44	15.6
	Cd	0.67	0.0
	Ni	0.75	22.8
Ga	Mn	0.2	0.0
	Cd	0.1	0.0
	Mg	0.7-0.8	0.0
	Co	0.86	2.1
	Fe	1.0	3.9
	Cu	1.0	15.6
	Ni	1.0	22.8
Mn	Zn	0.0	−25.3
	Cd	0.0	−25.3
	Co	0.0-0.2	−23.2
	Mg	0.0-0.4	−25.3
	Cu	0.2-0.4	−9.7
	Ni	0.74	−2.5
	V	0.8	0.0
	Fe	0.9	−21.4
	Ti	1.0	0.0
	Sn	1.0	0.0
	Cr	1.0	46.7

[a] $x = 0$ for a normal spinel, $x = 1.0$ for an inverse spinel, $x = 0.67$ for a random spinel. CFSE are calculated for oxide spinels only. [b] Most cases have a temperature-dependent value of x.

As a comparison of the quality of separation achieved in Figure 1, we mention sorting[15] using analogous parameters for the AB octet binaries (e.g., CuCl, ZnS, SiC, LiI). For a data base of 100 examples, the sorting is perfect by coordination number with two minor errors in that two compounds with the sphalerite (zincblende) structure fall in the wurtzite region. (These two structures with the same coordination numbers only differ at the third nearest-neighbor level!) With a data base of 95 octets, application of the traditional radius ratio rule ideas, using crystal radii appropriate for the observed coordination number (which, of course, we do not know in advance[16]), leads to 38 errors. Radius ratio rules are therefore an exceedingly poor way to predict structures. For 16-electron AB_2 systems a similar clean structural sorting is achieved using[15] r_σ^A, r_σ^B or χ^A, χ^B. Such "Mendelevian" approaches[7b,10g] are clearly of some utility.

It makes relatively little difference to the spinel diagram of Figure 1 if the radii $r_\sigma' = r_s + r_p + r_d$ are used as indexes (r_s, r_p are always bigger than r_d), but extremely poor sorting is found if an electronegativity, χ, is used which includes r_d^{-1}. The sorting is therefore achieved by using s and p functions only on the metals. This is in direct contrast to the CFT, of course, where s and p effects are ignored and d orbitals alone are used.

(11) See especially ref 10e and 10g.

(12) Hahn, H.; Klinger, W. *Z. Anorg. Allg. Chem.* **1950**, *263*, 177.
(13) Verwey, E. J. W.; Heilman, E. L. *J. Chem. Phys.* **1947**, *15*, 174.
(14) (a) König, U.; Chol, G. *J. Appl. Crystallogr.* **1968**, *1*, 124. (b) Huang, C.-H.; Knop, O. *Can. J. Chem.* **1971**, *49*, 598.
(15) Burdett, J. K.; Price, G. D.; Price, S. L. *Phys. Rev. B* **1981**, *24*, 2903.
(16) This figure of 38 errors is therefore the very best we can achieve. If average radii are used the number of errors is larger.

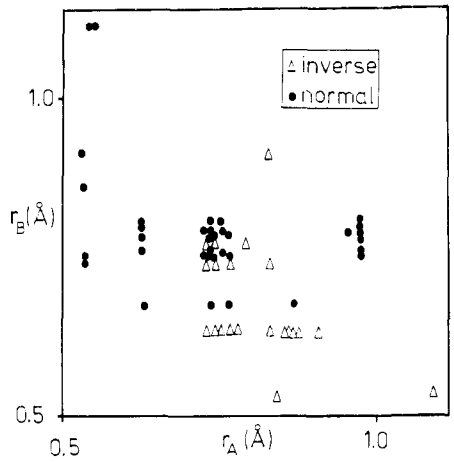

Figure 2. Structural sorting map for AB_2X_4 spinels using Shannon and Prewitt crystal radii r_A, r_B as indexes.

Apart from the gross sorting aspect of Figure 1, there are some other observations which are very interesting. That the boundary line separating normal and inverse structures is a realistic one is indicated by the fact that the borderline examples are often partially disordered with varying "amounts" of normal and inverse character. Table II shows how the crystal-field theory would treat these cases. A clear and obvious conclusion from these figures is that, in this borderline region, the d orbital forces *are* of importance in determining the structure. At the borderline a larger OSPE for B, compared to A, tends to stabilize the normal structure, and a smaller OSPE for B than A will stabilize the inverse structure. Away from this region, the crystal-field predictions are sometimes right and sometimes wrong, and often inapplicable.

We noted above that $r_s + r_p$ is strongly correlated with the Pauling tetrahedral radius. Can crystal radii (e.g., those of Shannon and Prewitt[17]) be used as indices to sort structures? One major problem is that these radii are coordination-number dependent and so the answer needs to be known before the plot may be made. Even with this information the sorting is not very good (Figure 2). The data base is much smaller than that used before (Table II) since for many ions suitable radii are not tabulated. Parenthetically we note the good structural sorting of AB_2O_4 compounds in general if crystal radii are used as indices[2a] and the data base is judiciously chosen.

Discussion

There are two very important questions raised by Figure 1. Firstly, the basic sort is achieved by using r_s and r_p only. Inclusion of r_d is practically inconsequential in these r_σ plots but destroys the good sorting if included in the χ plots. Secondly the number of d electrons associated with the A,B ions does not appear as a parameter. Compare these results with those expected from CFT considerations, namely, both a d orbital and electronic configuration dominated description.

In order to understand these striking results we need to look more closely at the transition metal–ligand interaction itself. Many of the effects ascribed to crystal-field splittings over the years are simply understood by using symmetry ideas alone.[18,19] Because *by symmetry* the atomic nd levels are split into $e_g + t_{2g}$ sets on octahedral coordination, the double-humped curves associated with a variety of properties (metal–oxygen distances, heats of hydration, lattice energies, rates of water loss from hexaquo ions) naturally follow. Identical answers result[18,20] (but with different explanations) if the CFT is used to give CFSE's, or a molecular orbital approach (we have pioneered[20-22] the use of the angular overlap

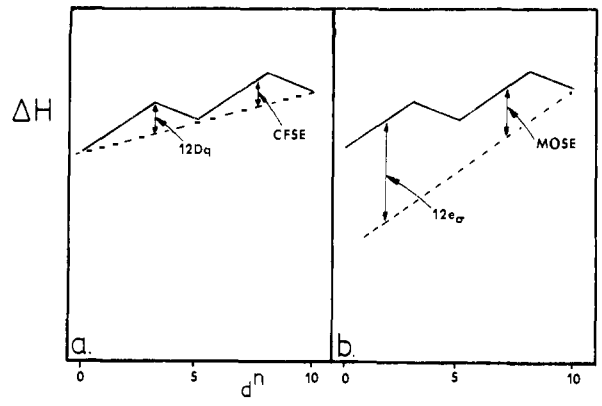

Figure 3. Comparison of (a) crystal-field and (b) angular-overlap treatment of the variation in heat of hydration of the first-row d^n ions.

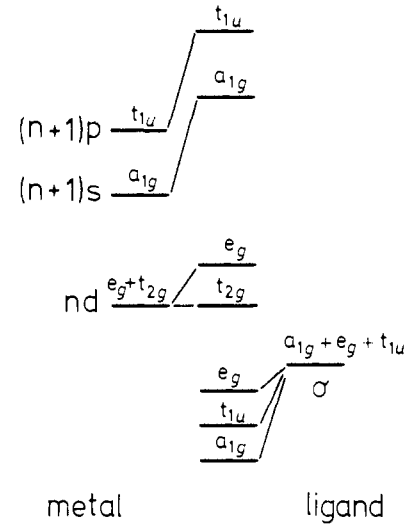

Figure 4. Molecular orbital diagram for an octahedral MX_6 complex showing interaction of the ligand σ orbitals with the metal s, p, and d orbitals.

model in this area) to give MOSE's (molecular orbital stabilization energies). Figure 3 shows the different descriptions of the heat of hydration variations[18,4b] as the number of d electrons changes. The sloping background in Figure 3b, often more than 90% of the total energy, is ascribed[22] to the contribution to the stabilization energy from ligand interactions (Figure 4) with metal $(n + 1)$ s,p orbitals. Energetically then the d orbital contribution, whether in terms of MOSE or CFSE, is rather small compared to the s,p contribution and a priori we would expect that site preferences [A][B] or [A]{B} should be primarily determined by the latter. Figure 1 indicates that this is indeed the case.

Our results have put the CFSE in its place. It was clear in the 1950's that there were indeed site preference energies for the nontransition metal ions, such as Al^{3+} for octahedral sites and Zn^{2+} for tetrahedral sites. The competition between Ni^{2+} and Al^{3+} shows that Al^{3+} has a greater octahedral site preference energy than Ni^{2+} and well illustrates the presence of factors other than the CFSE which strongly influence the problem. The nature of these "other factors" has remained elusive until now. Over the intervening years, however, the off-quoted caveat[9] that the CFSE "contributes only 5–10% of the total bonding energy" has often been forgotten, and crystal-field theory was used alone to view many aspects of transition metal chemistry despite the cautionary notes concerning such usuage which have appeared.[22,23] It is also interesting to note in this context too that, although the OSPE,

(17) Shannon, R. D., *Acta Crystallogr. Sect. A* **1976**, *32*, 751.
(18) Burdett, J. K. "Molecular Shapes", Wiley: New York, 1980.
(19) Gerloch, M.; Slade, R. C. "Ligand Field Parameters"; Cambridge University Press: New York, 1973.
(20) Burdett, J. K. *Adv. Inorg. Chem. Radiochem.* **1978**, *21*, 113.
(21) See also the discussion in DeKock, R. L.; Gray, H. B. "Chemical Structure and Bonding"; Benjamin Cummings: Menlo Park, 1980.
(22) Burdett, J. K. *J. Chem. Soc., Dalton Trans.* **1976**, 1725.
(23) Katzin, L. I. *J. Chem. Phys.* **1961**, *35*, 467; **1962**, *36*, 3034.

derived in terms of the CFSE's, gives a reasonable sorting of the cases where it is applicable (Table I), use of MOSE's alone does not give as good a picture.[22]

A structural sorting using the χ^A, χ^B indexes is understandable in terms of current ideas concerning site preference energies in molecules.[18,24] Given a set of atomic charges $\{q_i^\xi\}$ for the orbitals i (s, p, d) located on the symmetry inequivalent atoms (ξ) in a structure, the total energy will depend on the function $\sum_{i,\xi} q_i^\xi H_{ii}^\xi$, where H_{ii}^ξ is the relevant valence orbital ionization potential. The most stable structure will be the one with optimal matching of $\{q_i^\xi\}$ and $\{H_{ii}^\xi\}$ to give the lowest energy. In general, this will occur when the most electronegative atoms (largest H_{ii}) occupy the sites of highest charge. Since energetically they are more important than ligand–metal d interactions, the ligand–metal s,p interactions should analogously control the charge distribution and hence the site preferences. The gross structural sorting is then explicable in principle on these grounds, although, at present, we do not understand the exact location of the dividing lines. In addition, because of the impotence of d orbitals in determining these preferences, we can see why the number of electrons in these orbitals is immaterial in the display of Figure 1 (but, of course, vital to a CFT discussion). The finer details of the structures close to the boundaries, where the CFT methodology does appear to dominate, are also much more in keeping with the general idea that the d-orbital effects are small compared to s and p ones in this area.

An additional point concerning the relative sizes of the two types of interactions is associated with Jahn–Teller distortions in Cu^{II}- and Mn^{III}-containing spinels. These are best viewed as structural perturbations of the spinel structure itself, rather than leading to the generation of a completely different structural type. Such Jahn–Teller effects also appear to give rise to a relatively small structural perturbation in AB_2 systems[15] when viewed via structural mapping.

Although we have perhaps downplayed the importance of d orbitals and their occupation in this paper, it is vital to recognize that this view has only been advanced for the coordination number problem. There is ample evidence that this manifold of orbitals[25] and their electron occupancy is of tremendous importance in controlling angular geometry, relative bond lengths, ligand site preferences, reactivity, and many other facets of molecular structure.[18]

Finally it will be interesting to see if these ideas, developed for solids, can be extended to the molecular area. In recent years, most progress in understanding the structures of solids has resulted from the flow of ideas in the reverse direction.[26,27]

Acknowledgment. We thank the donors of the Petroleum Research Fund administered by the American Chemical Society for their partial support of this research and the National Science Foundation for their support under Grants NSF DMR 8019741 and NSF CHE 7826579. We also acknowledge useful discussion and correspondence with D. S. McClure.

Registry No. $FeAl_2O_4$, 12068-49-4; $MgAl_2O_4$, 1302-67-6; $CoAl_2O_4$, 1333-88-6; $MnAl_2O_4$, 12068-52-9; $CuAl_2O_4$, 12042-92-1; $CdAl_2O_4$, 12252-16-3; $NiAl_2O_4$, 12004-35-2; $MnGa_2O_4$, 12064-15-2; $CdGa_2O_4$, 12139-12-7; $MgGa_2O_4$, 12064-13-0; $CoGa_2O_4$, 12139-60-5; $FeGa_2O_4$, 12062-71-4; $CuGa_2O_4$, 12053-83-7; $NiGa_2O_4$, 12064-17-4; $ZnMn_2O_4$, 12163-55-2; $CdMn_2O_4$, 12050-21-4; $CoMn_2O_4$, 12139-69-4; $MgMn_2O_4$, 12163-24-5; $CuMn_2O_4$, 12019-04-4; $NiMn_2O_4$, 12057-90-8; VMn_2O_4, 12163-54-1; $FeMn_2O_4$, 12332-30-8; $TiMn_2O_4$, 12032-93-8; $SnMn_2O_4$, 12209-43-7; $CrMn_2O_4$, 12410-51-4.

(24) Hoffmann, R.; Howell, J. M.; Muetterties, E. L. *J. Am. Chem. Soc.* **1976**, *98*, 2484.

(25) Although we traditionally call these "d orbitals", if the local symmetry is lower than cubic, then they will in fact contain admixture of s and p orbitals. In this sense then higher energy orbitals also play a crucial role in determining even these properties.

(26) See, for example, the articles in ref 7c.

(27) Burdett, J. K. *Nature London* **1979**, *279*, 121.

Structures of $[(Ph_3C_3)M(PPh_3)_2]^+X^-$ Complexes. An Experimental and Theoretical Study of Ring-Whizzing

Carlo Mealli,[1a] Stefano Midollini,[1a] Simonetta Moneti,[1a] Luigi Sacconi,*[1a] Jerome Silvestre,[1b] and Thomas A. Albright*[1b,c]

Contribution from the Instituto di Stereochimica di Coordinazione del C.N.R., Instituto di Chimica Generale e Inorganica dell' Universita', 50132 Firenze, Italy, and the Department of Chemistry, University of Houston, Houston, Texas 77004. *Received February 27, 1981. Revised Manuscript Received August 15, 1981*

Abstract: Complexes of the formula $[(Ph_3C_3)M(PPh_3)_2]X$, where M = Ni, Pd and X = ClO_4, PF_6, have been prepared by the reaction of (ethylene)$M(PPh_3)_2$ with triphenylcyclopropenium perchlorate or hexafluorophosphate. Complete X-ray analysis has been carried out for $[(Ph_3C_3)Ni(PPh_3)_2]PF_6$ (**1**), $[(Ph_3C_3)Pd(PPh_3)_2]ClO_4$ (**2**), and $[(Ph_3C_3)Pd(PPh_3)_2]PF_6 \cdot C_6H_6$ (**3**). The crystal data are as follows: (**1**) a = 15.815 (4) Å, b = 13.781 (4) Å, c = 12.764 (4) Å, α = 114.06 (9)°, β = 95.92 (9)°, γ = 97.74 (9)°, Z = 2, space group $P\bar{1}$; (**2**) a = 11.115 (4) Å, b = 35.486 (9) Å, c = 12.584 (4) Å, β = 104.49 (7)°, Z = 4, space group $P2_1/n$; (**3**) a = 12.130 (5) Å, b = 23.863 (7) Å, c = 18.669 (6) Å, β = 91.45 (8)°, Z = 4, space group $P2_1/n$. The structures were refined to R values 0.079, 0.079, and 0.065 for **1**, **2**, and **3**, respectively. These three structures, along with a previously determined one where M = Pt, X = PF_6, **4**, show a progressive movement of the $(Ph_3P)_2M$ unit over the face of the cyclopropenium cation. In other words, these structures chart the reaction path for going from one η^2 geometry, where the $(Ph_3P)_2M$ unit is positioned below one carbon–carbon bond, to an equivalent η^2 geometry. The movement of the $(PPh_3)_2M$ group is accompanied by rotation, as well as a number of other geometrical changes. A potential surface for this ring-whizzing motion was determined by molecular orbital calculations of the extended Hückel type. The calculations mimic the geometrical details experimentally found and provide an electronic rationale for the observed distortions. The calculations and observed structures are in agreement with the McIver–Stanton theorem which regulates the symmetry of potential surfaces. The effect of substitution on the cyclopropenium ring and of changing the phosphines to other ligands on the potential surface is also discussed.

Ring-Whizzing, a type of fluxionality where an ML_n unit migrates inside the periphery of a cyclic polyene, has been extensively studied by NMR methods.[2] Activation energies throughout the entire range of dynamic NMR (ca. 7–22 kcal/mol)

0002-7863/82/1504-0095$01.25/0